# Typhoon at CommsNet13: experimental experience on AUV navigation and localization

**B. Allotta** [*,**] **F. Bartolini** [**] **A. Caiti** [*,***] **R. Costanzi** [**]
**F. Di Corato** [****,1] **D. Fenucci** [***] **J. Gelli** [**] **P. Guerrini** [†]
**N. Monni** [**] **A. Munafò** [†] **M. Natalini** [**] **L. Pugi** [**] **A. Ridolfi** [**]
**J.R. Potter** [†]

[*] *ISME Interuniversity Res. Ctr. on Integrated Systems for the Marine Environment (e-mail: andrea.caiti@unipi.it)*
[**] *DIEF Dept. Industrial Engineering, University of Florence, Florence, Italy (e-mail: benedetto.allotta@unifi.it)*
[***] *DII & Centro Piaggio University of Pisa, Pisa, Italy (e-mail: andrea.caiti@unipi.it)*
[****] *Magneti Marelli S.p.A. - ADAS Technologies, CTO, Venaria (TO), Italy (email: francesco.dicorato@magnetimarelli.com)*
[†] *CMRE NATO STO Ctr. for Maritime Research and Experimentation, La Spezia, Italy (e-mail: john.potter@cmre.nato.int)*

**Abstract:** This paper presents two acoustic-based techniques for Autonomous Underwater Vehicle (AUV) navigation within an underwater network of fixed sensors. The proposed algorithms exploit the positioning measurements provided by an Ultra-Short Base Line (USBL) transducer on-board the vehicle to aid the navigation task. In the considered framework the acoustic measurements are embedded in the communication network scheme, causing time-varying delays in ranging with the fixed nodes. The results presented are obtained with post-processing elaborations of the raw experimental data collected during the CommsNet13 campaign, organized and scientifically led by the NATO Science and Technology Organization Centre for Maritime Research and Experimentation (CMRE). The experiment involved several research institutions and included among its objectives the evaluation of on-board acoustic USBL systems for navigation and localization of AUVs. The ISME groups of the Universities of Florence and Pisa jointly participated to the experiment with one Typhoon class vehicle. This is a 300 m depth rated AUV with acoustic communication capabilities originally developed by the two groups for archaeological search in the framework of the THESAURUS project. The CommsNet13 Typhoon, equipped with an acoustic modem/USBL head, navigated within the fixed nodes acoustic network deployed by CMRE. This allows the comparison between inertial navigation, acoustic self-localization and ground truth represented by GPS signals (when the vehicle was at the surface).

*Keywords:* AUV (Autonomous Underwater Vehicle), acoustic networks, navigation, positioning systems

## 1. INTRODUCTION

In the last decades the advances in underwater robotics has significantly grown, leading to the development of new technologies and methodologies in the marine area. However, navigation and self-localization are still challenging tasks for the AUVs due to the tight constraints imposed by the acoustic channel, such as the absence of a global positioning system. A thorough review on different strategies that have been investigated and validated with experimental tests through the years is reported in Paull et al. (2014) and references therein. As there shown, the navigation task is generally mission-oriented: depending on the specific application, the equipment on-board the vehicle and the required navigation accuracy change, defining a trade-off between performance and cost. Basically, unaided Inertial Navigation System (INS) provides information that allow to continuously calculate the vehicle position, velocity and orientation via dead-reckoning. As it is well known, this procedure is subject to cumulative errors due to the INS inaccuracies. High-precision inertial units have a cost that can reach and overcome 1 Million €; for this reason, they are suitable for operations with a single, high-performance vehicle. In applications where the need of keeping the cost of any individual vehicle within reasonable bounds is strong (i.e. environmental exploration with a team of AUVs), the use a low-cost,

[1] Work done when the author was at Interuniversity Res. Ctr. on Integrated Systems for the Marine Environment, DII & Centro Piaggio, University of Pisa.

industrial grade INS is more appropriate. However, such units may lead to typical horizontal drifts of 50 - 60 m per minute VectorNav Technologies LLC (2014). As a consequence, these systems require a procedure able to compensate the error drift of the on-board INS by integrating measurements from other navigation aids, i. e. Doppler Velocity Log (DVL), depth sensor, acoustic positioning systems. In particular, a growing attention is being paid to acoustic positioning in the form of Long Base Line (LBL) or USBL systems for underwater robots, see for instance Furfaro and Alves (2014); Morgado et al. (2013); Batista et al. (2012); Webster et al. (2012). With the adoption of these systems, Simultaneous Localization And Mapping (SLAM)-like techniques developed for ground robotics can be applied to the underwater domain by exploiting the acoustic positioning information. For instance, in Petillot et al. (2010) a range-only SLAM algorithm has been tested with simulations, while Becker et al. (2012) propose a SLAM-like approach with a single transponder used as landmark.

In this work we present the experimental results obtained with two techniques for navigating an AUV within an acoustic sensors network by using a mixed USBL/LBL system. In the first approach, the vehicle employs the USBL measurements first to localize the fixed nodes of the network and then to perform autonomous navigation. The second technique aims at simultaneously estimate both the navigation of the vehicle (i.e. its position and velocity) and the topology of the network by using the acoustic measurements; given the similarity with the classical SLAM problem, we named this framework *Acoustic-based SLAM (A-SLAM)*. The peculiarity of the proposed strategies lies in the fact the acoustic positioning information are embedded in a networked communication scheme. As a consequence, the presented algorithms can be extended without considerable efforts to support a multi-vehicle cooperative navigation framework.

The vehicle considered in this work belongs to a new class of AUVs, called Typhoon, able to cooperate in swarms to perform navigation, exploration and surveillance of underwater archaeological sites and developed in the framework of the THESAURUS project (Italian acronym for "TecnicHe per l'Esplorazione Sottomarina Archeologica mediante lUtilizzo di Robot aUtonomi in Sciami", 2010-2013). The project specifications were quite ambitious: the developed low cost vehicles have to operate with a maximum depth of 300 m, an autonomy ranging from 8 to 12 hours is required and a maximum speed of 5-6 knots has to be achieved. Briefly, the Typhoon class AUV is a vehicle with remarkable performances and power on-board. In particular, it is worth to note that the depth specification is very significant for archaeological interests: the depth of 300 m is prohibitive for usual diver operations and it is also higher compared to the depth specification of many commercial low cost AUVs. The total carried payload is quantified in about 30-40 kg.

A first fleet of three different underwater vehicles has been developed, to cooperate as a single team, as envisaged in Figure 1: see Allotta et al. (2013, 2014). The three vehicles can be characterized as follows.

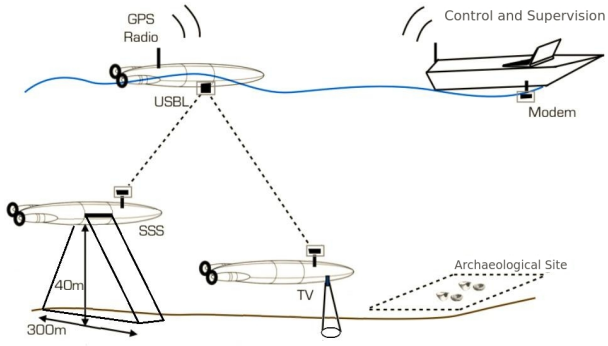


Figure 1. Typhoon AUVs of the swarm

**Vision Explorer** A vehicle equipped with cameras, lighters and structured laser light for an accurate visual inspection and surveillance of archaeological sites. The visual inspection involves a short range distance (few meters) between the vehicle and the target site, and the capability of performing precise manoeuvring and hovering;

**Acoustic Explorer** Preliminary exploration of wide areas to recognize potentially interesting sites involves the use of acoustic instruments, such as side-scan-sonar. This kind of vehicle can perform long range missions. Consequently, navigation sensors able to compensate the drift of the inertial sensors, such as a DVL, have to be installed on board;

**Team Coordinator** A vehicle with extended localization and navigation capabilities is used to coordinate the team. This vehicle periodically returns to surface getting the GPS position fix and, more generally, detailed navigation information that can be shared with other vehicles of the team. Currently the authors have adopted the following approach: when the mission area is quite defined and a surface vehicle or a buoy are available, coordination and data transmission are performed by this dedicated device. On the other hand, when a different operating scenario is required, one or more vehicles of the team could periodically interrupt their mission performing the activity of team coordinator.

Each vehicle of the team can be customized for different mission profiles; moreover the team composition can be altered, e.g. two vehicles may be equipped for the visual inspection of a site. Since each vehicle differs only in terms of sensor layout and payload, the naval and the electromechanical design was focused on a common vehicle class. For an individual mission in which both acoustic and visual inspection of an archaeological site are performed by a single vehicle the instrumentation layout described in Figure 2 can be easily assembled (housing optical cameras and acoustic payload, for instance a Side-Scan Sonar (SSS)). Following extensive engineering tests, that took part in summer 2013 within the THESAURUS project activities, one of the Typhoon vehicle, operated by the ISME (Interuniversity Centre of Integrated Systems for the Marine Environment) groups of the Universities of Florence and Pisa, participated in the CommsNet13 experiment, organized by the NATO CMRE in September 2013. The Typhoon vehicles are also part of the heterogeneous fleet of AUVs of the ARROWS European project (`www.arrowsproject.eu`).

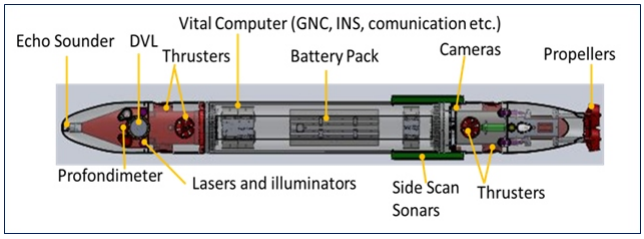


Figure 2. A Typhoon vehicle customized for both acoustic and visual inspection of a site

In the following we present the main features of the Typhoon AUV, a mathematical formulation of the proposed navigation approaches and the results obtained off-line by running the algorithms on the data collected during the CommsNet13 experiment.

## 2. MAIN FEATURES OF THE TYPHOON VEHICLE

Typhoon vehicle is a middle-sized class AUV. Considering the vehicle sizes (length of 3600 mm, external diameter of 350 mm, weight of 130-180 kg according to the carried payload) and the expected performances (maximum reachable depth of about 300 m, at least 10-12 hours of autonomy and a maximum speed of 5-6 knots) the vehicle can be considered an intermediate one compared to the smaller Remus 100 and the bigger Remus 600. At the moment, two Typhoons AUVs already performed many missions at sea: the vehicles are called TifOne and TifTu (Italian pronunciation of TifTwo). TifTu has no payload on-board and usually navigates on surface. It mounts an USBL acoustic head useful to relatively localize TifOne when the latter navigates underwater. The adopted configuration in the THESAURUS project is that the transceiver (USBL) is located on a surface support vehicle (i.e. TifTu or a support ship); the transponder is instead an acoustic modem rigidly mounted on-board of one of the AUVs navigating underwater (i.e. TifOne). The Typhoon AUVs (TifOne and TifTu) participated in the CommsNet13 experiment, organized and led by NATO Science and Technology Organization Centre for Maritime Research and Experimentation, in La Spezia (Italy). In Figure 3 the Typhoon CAD design and its final built versions (TifOne and TifTu) can be seen.

Both TifOne and TifTu are moved by propellers. The propulsion system is composed of six actuators: two lateral thrusters, two vertical thrusters and two main rear propellers. The propulsion system actively controls five degrees of freedom of the vehicle, the only one left passive being the roll one. A standard actuation unit with a 200 W brushless motor and drive directly fed by the 48 V provided by the batteries and controlled through an industrial CAN bus has been adopted (Carlton, 2012). The calibration of the pitch static attitude can be also performed by moving the accumulators whose axial position is controlled by a screw system. For sake of brevity, here is only reported a list of the on board sensors and payloads:

- Inertial Measurement Unit (IMU) Xsens MTi: device consisting of a 3D gyroscope, 3D accelerometer and 3D magnetometer furnishing (at 100 Hz) the orientation of the vehicle in a 3D space;

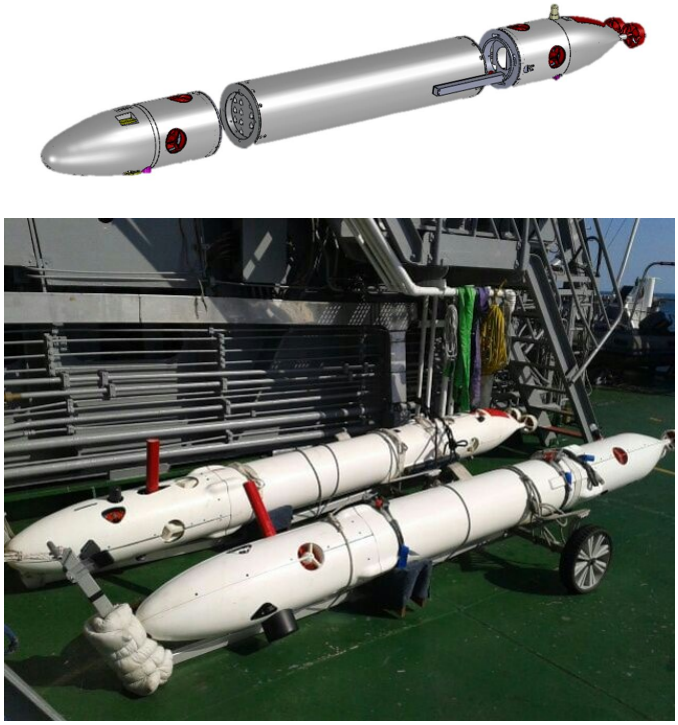

Figure 3. Typhoon AUVs: CAD design (top) and final versions on the NATO Research Vessel Alliance, during CommsNet13 (bottom).

- Doppler Velocity Log (DVL) Teledyne Explorer (on TifOne): sensor measuring the velocity of the vehicle, with respect to the seabed;
- Echo Sounder Imagenex 852: single beam sensor, pointing forward and measuring the distance from the first obstacle placed in front of the vehicle;
- STS DTM depth sensor: digital pressure sensor used to measure the vehicle depth;
- PA500 altimeter: echo-sounder measuring the distance of the vehicle from the seabed;
- Optical cameras ace by Basler (on TifOne): optical stereo cameras for a detailed visual inspection of the targets;
- SeaKing 675 kHz SSS by Tritech (on TifOne): for the acoustic survey of the seabed;
- S2CR 18/34 Underwater Acoustic Modem by EvoLogics (on TifOne): acoustic device for the underwater communication;
- S2CR 18/34 USBL Underwater Acoustic USBL System by EvoLogics (on TifTu): device for the underwater acoustic localization. The USBL is fundamental for the geo-localization of the vehicle navigating underwater and thus also for geo-referencing the acquired data.

### *2.1 Acoustic Communication*

As mentioned in the Introduction, the acoustic communication system has been designed having in mind an operation with a team of Typhoon vehicles. To this aim, the vehicles have to establish a communication network based on a time-sharing bi-directional/broadcast scheme. The goal is to create a flexible structure capable of ensuring

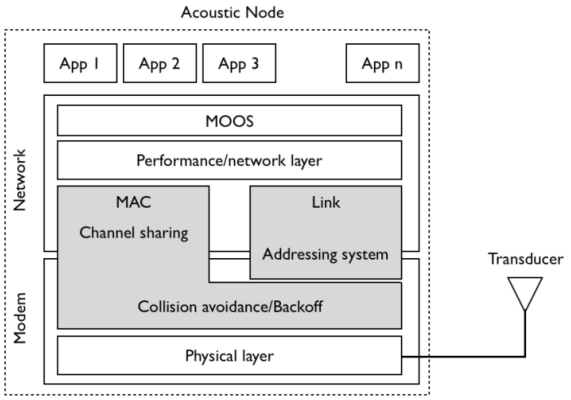


Figure 4. Layered structure of the underwater acoustic network

low-delay communication and the reliable transmission of specific messages necessary for the safety of the swarm and for exploration missions. The network is composed of a few layers, as shown in Figure 4, and it does not include most of the complexity typically present in terrestrial networks. The implemented networking system has already been described in Caiti et al. (2013). Its main features are reported here for self-consistency. The bottom layer is represented by the EvoLogics acoustic modem/USBL, which manages the physical transmission of the signal into the water. The adopted communication mode provided by the modem, namely instant messaging, does not require connection establishment procedures, allows for broadcast messaging and permits a message maximum size of 64 bytes. The modem also implements collision avoidance techniques, i.e. Medium Access Control (MAC), and provides basic network functionalities, including an addressing system that can be exploited at the link layer. The medium access control is completed through a Time Division Multiple Access (TDMA) mechanism: time is divided into slots and to each node a slot where it has to concentrate all its communication burden is assigned. The network link layer is composed of a combination of the modem networking features and of the Mission Oriented Operating Suite (MOOS) framework (Newman, 2003). MOOS is a publisher/subscriber system for inter-process communication through message exchange. Messages are associated to an information descriptor, called *topic*, contained in the messages themselves. Publishers send their messages to a dispatcher, represented by a central database (MOOSDB), which is responsible for forwarding messages to the subscribers based on their topic. Subscribers have to preliminary declare their interest in specific topics by issuing subscription to the dispatcher itself. Within this setting, each acoustic node is equipped with a process that handles the communication with the acoustic device: when a new message is received from the modem, it publishes the information in the INBOX topic, whereas during a transmission, it reads a message from the OUTBOX topic and forwards it to the modem for the physical transmission. To increase the throughput of the network and the probability that an important message is transmitted as soon as possible, messages are organized in a priority queue. More specifically, four classes of messages have been identified, each of which associated with a decreasing priority; among them, the localization messages, periodically exchanged between the vehicles to have USBL updates or range measurements, are relevant to the aim of CommsNet13 experiment. To avoid an indefinitely growth of the queue when an application generates data at a higher rate than the acoustic channel can support, at each step the messages are filtered on the basis of the time slot duration and those that cannot fit into the available time are discarded. Finally, the network link layer also includes an additional sub-layer, namely the performance/network layer, used to adapt the requests coming from the application level to the constraints of the layers below it and of the acoustic channel. The highest layer, namely the application layer, utilizes MOOS as software infrastructure. An application which wants to join the network has only to publish in the topic OUTBOX the data to be sent acoustically towards the desired nodes and to register to the topic INBOX to be notified when new acoustic messages are received. This way, the network becomes completely transparent from the application point of view.

## 3. NAVIGATION ALGORITHMS

In this section, we give an overview of the proposed navigation strategies with a hybrid USBL/LBL system. We consider an AUV navigating within a network of $N_m$ fixed acoustic transponders, i.e. the LBL, deployed in initially unknown positions $\boldsymbol{p}_{m_i}$, $i = 1, \ldots, N_m$. The vehicle is supposed to be equipped with a low-cost, low-accuracy IMU aided by a set of navigation devices, namely a GPS receiver, a depth sensor and an USBL modem, which can communicate with the nodes of the network and obtain localization information. In particular, the USBL provides, when possible, the module and the orientation of the distance of the considered transponder with respect to itself by interrogating it and waiting for the synchronized answer. The relative position is thus provided as a vector resolved in the USBL own reference frame $\{u\}$. The module of the vector is calculated on the basis of the round-trip time of the message and the speed of sound into the acoustic channel. The orientation, instead, is estimated from the phases of the signal received back by each transducer constituting the USBL head. While travelling, the vehicle periodically interrogates all the LBL anchors sequentially, obtaining for each of them a cluster of raw measurements to enhance the navigation system. Note that such communication protocol complies with the one designed within the THESAURUS project and described in section 2.1. Furthermore, as all time-division networking protocols, it introduces non-negligible delays and overhead through the network; hence, the acoustic positioning measurements will arrive at a much lower rate than the other sensors acquirements.

For the purposes of this work, given the mission scenario, we can make some assumptions to simplify the problem. First, since the motion of the vehicle was assumed to be enclosed inside a bounded, *small enough* area, we approximate the Earth as a flat surface in the neighbourhood of the starting point. This means that the local navigation frame $\{n\}$, defined in North-East-Down (NED) coordinates, does not change its orientation with respect to the global Earth-Centered, Earth-Fixed (ECEF) frame during the whole navigation task. As a consequence, by defining

the origin of the NED reference frame on the Earth surface at the location corresponding to the starting point, all the inertial quantities can be considered in local coordinates. Moreover, we assume that the IMU is placed in the Centre Of Gravity (COG) of the vehicle with the axes directed along the corresponding axes of the body-fixed reference system $\{b\}$ defined according to Fossen (1994). On the other hand, the alignment of the USBL frame $\{u\}$ with respect to the frame $\{b\}$ is considered to be known. In particular, the USBL is supposed to be mounted with an arbitrary orientation with respect to the body-fixed frame and the misalignment is expressed through the constant transformation matrix ${}^{b}\mathbf{R}_{u}$. The accurate estimation of the mounting matrix of a device can be a critical point. In the underwater context, a peculiar factor for the performance of the vehicle navigation is generally the calibration of the DVL frame with respect to the body-fixed axes. Many approaches to obtain an on-line estimation of the DVL misalignment can be found in literature (Di Corato et al., 2015; Tang et al., 2013), also with a detailed error analysis (Kinsey and Whitcomb, 2007). The calibration of the USBL is less critical: indeed, any eventual error does not introduce a drift in the position estimation, but at most a constant bias. However, a detailed analysis on the effects of any eventual error in the USBL-to-body matrix estimation is beyond the scope of this work.

Finally, the orientation of the vehicle is assumed known. More specifically, the orientation $\boldsymbol{\Theta}$, parametrized with Euler angles, is estimated by the inertial unit on-board the vehicle, via integration of the gyroscopes measurements together with the sensed gravity and the Earth magnetic field measurements in an Attitude and Heading Reference System (AHRS) fashion.

### *3.1 Two-phases navigation*

This approach is conceptually composed of two consecutive steps. The first one, namely the *fixed-nodes localization*, aims to find out the topology of the LBL. Once the absolute position of the anchors has been determined, the second phase, namely the *acoustic-aided navigation*, can start: the vehicle exploits the acoustic measurements together with the information about the network previously obtained to enhance its navigation system. In the following we will detail both the phases.

*Fixed-nodes localization* In this phase the AUV navigates on surface, thus having the continuous availability of the GPS signal, which can be modelled as follows:

$$\tilde{\boldsymbol{y}}_{\text{gps}} = \boldsymbol{p}_{\text{gps},n} + \boldsymbol{\eta}_{\text{gps}} \tag{1}$$

where $\boldsymbol{p}_{\text{gps},n} \in \mathbb{R}^2$ contains the North-East components of the vehicle absolute position and $\boldsymbol{\eta}_{\text{gps}} \sim \mathcal{N}(\mathbf{0}, \boldsymbol{R}_{\text{gps}})$ is a white, Gaussian noise with zero mean and constant covariance matrix $\boldsymbol{R}_{\text{gps}}$. In the following, unless otherwise specified, we will always denote with the symbol "$\eta_{\text{dev}}$" a noise with such characteristics associated to the device *dev*.

During the navigation, the vehicle starts interrogating in sequence all the modems constituting the network using the on-board USBL. Any measurement acquired from the $i$-th LBL anchor can be modelled as follows:

$$\tilde{\boldsymbol{y}}_{\text{usbl}_\text{i}} = \boldsymbol{p}_{\text{m}_\text{i}\text{-u},u} + \boldsymbol{\eta}_{\text{usbl}} \tag{2}$$

where $\boldsymbol{p}_{\text{m}_\text{i}\text{-u},u} \in \mathbb{R}^3$ is the relative position of the $i$-th acoustic modem with respect to the USBL head and $\boldsymbol{\eta}_{\text{usbl}} \sim \mathcal{N}(\mathbf{0}, \boldsymbol{R}_{\text{usbl}})$ is the measurement noise associated to the USBL modem itself. The absolute position of the $i$-th node can thus be obtained by combining the USBL measurement with the absolute position of the vehicle at the same time instant $k$:

$$\boldsymbol{p}_{m_i,n}(k) = \begin{bmatrix} \tilde{\boldsymbol{y}}_{\text{gps}}(k) \\ 0 \end{bmatrix} + {}^{n}\mathbf{R}_{b}(\boldsymbol{\Theta}(k)) \, {}^{b}\mathbf{R}_{u} \tilde{\boldsymbol{y}}_{\text{usbl}_\text{i}}(k) \tag{3}$$

We remark that the relative position is resolved in the reference system $\{u\}$, thus it has to be compensated both for the mounting of the device and for the orientation of the vehicle at the corresponding time using the transformation matrices ${}^{b}\mathbf{R}_{u}$ and ${}^{n}\mathbf{R}_{b}(\boldsymbol{\Theta}(k))$, respectively.

This procedure is iterated several times, collecting for each node of the network a set of rough absolute position estimates with dimension $N_i$, $i = 1, \ldots, N_m$, not necessarily equal. Each cluster is then purged from any potential outlier (Indiveri, 2013) and the remaining elements are averaged in order to obtain a final estimate of the network topology:

$$\bar{\boldsymbol{p}}_{m_i,n} = \frac{1}{N_i} \sum_{j=1}^{N_i} \boldsymbol{p}_{m_i,n}(k_j), \quad i = 1, \ldots, N_m \tag{4}$$

We remark that as the dimension of a cluster increases the estimated absolute position of the corresponding node gets closer to the true one. Indeed, since the measurements are independent and unbiased (i.e. the associated noises have zero mean), the statistical mean will converge in probability to the expected value.

*Acoustic-aided navigation* Starting from the knowledge of the absolute position of the moored modems, the AUV can employ the acoustic measurements in a self-localization procedure by inverting the equation (3). The autonomous navigation algorithm here described relies on the strap-down inertial mechanization equations (Rogers, 2000). Usually, the input of such a navigation system is represented by the accelerometers measurement, which can be modelled as follows:

$$\tilde{\boldsymbol{u}}_{\text{acc}} = \boldsymbol{a}_b + \boldsymbol{\epsilon}_b - {}^{b}\mathbf{R}_{n}(\boldsymbol{\Theta})\boldsymbol{g}_n + \boldsymbol{\nu}_{\text{acc}} \tag{5}$$

where $\boldsymbol{a}_b$ and $\boldsymbol{\epsilon}_b$ denote respectively the actual dynamic acceleration of the vehicle and the sensors bias in the body-fixed reference frame $\{b\}$. The vector $\boldsymbol{g}_n$ represents the gravity in the navigation frame; note that, since the accelerometers sense the gravity acting along its axes, the vector $\boldsymbol{g}_n$ is transformed in the frame $\{b\}$ through the matrix ${}^{b}\mathbf{R}_{n}(\boldsymbol{\Theta}) = {}^{n}\mathbf{R}_{b}(\boldsymbol{\Theta})^{T}$. Finally, $\boldsymbol{\nu}_{\text{acc}} \sim \mathcal{N}(\mathbf{0}, \boldsymbol{Q}_{\text{acc}})$ is the measurement noise associated with the accelerometers.

Given the above hypothesis the classical formulation can be simplified, leading to the following *local* continuous-time model:

$$\dot{\boldsymbol{p}}_n = \boldsymbol{v}_n \tag{6a}$$
$$\dot{\boldsymbol{v}}_n = {}^{n}\mathbf{R}_{b}(\boldsymbol{\Theta})(\tilde{\boldsymbol{u}}_{\text{acc}} - \boldsymbol{\epsilon}_b + \boldsymbol{\nu}_{\text{acc}}) + \boldsymbol{g}_n \tag{6b}$$
$$\dot{\boldsymbol{\epsilon}}_b = \boldsymbol{\nu}_{\epsilon} \tag{6c}$$

where $\boldsymbol{p}_n$ and $\boldsymbol{v_n}$ are respectively the position and the velocity of the vehicle in the local navigation reference system $\{n\}$. Since no a-priori information is given about the nature of the bias time evolution, its dynamics is modelled in (6c) as a random walk, where $\boldsymbol{\nu}_{\epsilon} \sim \mathcal{N}(\mathbf{0}, \boldsymbol{Q}_{\epsilon})$ is a

zero-mean, white, Gaussian noise with constant covariance matrix.

Due to the network overburden induced by the communication protocol, the acoustic positioning fixes could arrive at largely spaced intervals of time. For this reason, being the USBL the only underwater navigation aid on-board the vehicle, we need a solution to keep the position error drift bounded in the time period between two consecutive acoustic measurements. We thus augment the outputs set with a *pseudo-measurement* of the velocity, built starting from the known desired thrust. For instance, assuming that the vehicle moves only along its own surge axis, we approximate the relation between the desired thrust and the velocity along that axis with the linear function

$$\tau_{\text{surge}} = K_{\text{thr}} v_{\text{surge}} \tag{7}$$

in which the gain $K_{\text{thr}}$ is supposed to be constant, or at least slightly variable, and initially unknown. The value of the gain can be estimated by extending the system model (6) with the following additional equation:

$$\dot{K}_{\text{thr}} = \nu_K \tag{8}$$

where $\nu_K \sim \mathcal{N}(0, Q_K)$ accounts for the model uncertainties. Although this is a very simplified approximation (i.e. it does not take into account environmental factors such as currents, wind, etc.), it is enough to make the position estimate not to diverge in the short term.

In order to reduce the intrinsic drift due to the integration of the sensed acceleration, the navigation procedure combines the state model evolution (6) and (8) together with the measurements from the other aiding sensors, generally considered as outputs. The GPS signal, whose model is given by (1), is used as a correction at the beginning of the mission to initialize the navigation algorithm, i.e. to make the accelerometers bias converge. Then, it is used in the experimentation described here as *ground truth* only, meaning that the navigation algorithm does not take advantage of the global localization system, thus simulating an underwater operation where GPS is not available. Note that in practical situations the GPS signal is integrated in the overall navigation system, when available (Caiti et al., 2013). The measurement equations associated to the remaining navigation aids, i.e. the USBL and the depth sensor, are respectively equation (2) and:

$$\tilde{y}_{\text{depth}} = p_{\text{depth},n} + \eta_{\text{depth}} \tag{9}$$

where $p_{\text{depth},n} \in \mathbb{R}$ is the Down coordinate of the vehicle position and $\eta_{\text{depth}} \sim \mathcal{N}(0, R_{\text{depth}})$ is the associated noise. Finally, the last navigation aid used in the algorithm is the allocated thrust along the surge axis of the vehicle, namely $\tau_{\text{surge},b}$, considering null the motion along the remaining two components. The relative equation is thus:

$$\tilde{\boldsymbol{y}}_\tau = [\tau_{\text{surge},b} \quad 0 \quad 0]^T + \boldsymbol{\eta}_\tau \tag{10}$$

where $\boldsymbol{\eta}_\tau \sim \mathcal{N}(0, \boldsymbol{R}_\tau)$ takes into account the model uncertainties and approximations. In order to fuse such measurements with the inertial navigation system, it is convenient to explicit the dependence of all the above measurements with respect to the vector of the inertial mechanization states $\boldsymbol{x} = \left[\boldsymbol{p}_n^T \ \boldsymbol{v}_n^T \ \boldsymbol{\epsilon}_b^T \ K_{\text{thr}}\right]^T$. Hence, the resulting output model of the system is:

$$\boldsymbol{y}_{\text{gps}} = [\boldsymbol{I}_2 \quad \boldsymbol{0}_{2\times N_s-2}]\,\boldsymbol{x} + \boldsymbol{\eta}_{\text{gps}} \tag{11a}$$

$$\boldsymbol{y}_{\text{usbl}_i} = {}^u\mathbf{R}_b\,{}^b\mathbf{R}_n(\boldsymbol{\Theta})\left(\bar{\boldsymbol{p}}_{m_i,n} - \boldsymbol{p}_n\right) + \boldsymbol{\eta}_{\text{usbl}} \tag{11b}$$

$$y_{\text{depth}} = [0 \quad 0 \quad 1 \quad \boldsymbol{0}_{1\times N_s-3}]\,\boldsymbol{x} + \eta_{\text{depth}} \tag{11c}$$

$$\boldsymbol{y}_\tau = K_{\text{thr}}\,{}^b\mathbf{R}_n(\boldsymbol{\Theta})\boldsymbol{v}_n + \boldsymbol{\eta}_\tau \tag{11d}$$

where $N_s$ is the state vector dimension. Equation (11b) expresses the USBL measurement by transforming the difference between the estimated positions of the $i$-th acoustic node and of the vehicle in the device frame $\{u\}$ through the transformation matrix ${}^u\mathbf{R}_b\,{}^b\mathbf{R}_n(\boldsymbol{\Theta})$. Note that the absolute position of the $i$-th acoustic modem $\bar{\boldsymbol{p}}_{m_i,n}$ is the corresponding one obtained with the procedure described in section 3.1.1. Furthermore, equation (11d) simply represents the relation (7) resolved in the body-fixed frame $\{b\}$.

The auxiliary measurements modelled by (1), (2), (9) and (10) are then fused together with the system dynamics described in (6) and (8) and the system output given by (11) through an Extended Kalman Filter (EKF). For the purposes of the filter implementation, each model is time-discretized via Euler integration method. Moreover, the navigation devices on-board the vehicle notify their own acquirements at different rates. Among these frequencies, the higher is generally associated to the inertial unit. For this reason, the filter runs at the IMU rate in order to exploit all the measurements. At each time instant $k$, the algorithm executes the classic Kalman *prediction step* (Jazwinski, 2007) to evaluate a rough estimate of both the navigation state $\boldsymbol{x}$ and the covariance matrix of the estimation error $\boldsymbol{P}$. After that, the predictions $\hat{\boldsymbol{x}}^-(k+1), \boldsymbol{P}^-(k+1)$ are refined in the *correction step* with the auxiliary measurements available at that time, to obtain the final estimates $\hat{\boldsymbol{x}}^+(k+1), \boldsymbol{P}^+(k+1)$.

### *3.2 Acoustic-based SLAM*

This approach aims to employ the acoustic measurements received through the channel in order to simultaneously estimate both the navigation of the vehicle (i.e. its position and velocity) and the topology of the network (i.e. the position of the fixed nodes), initially supposed unknown. In this framework, the LBL anchors are thus considered as *features* in a classic SLAM problem. Note that, in principle, this procedure represents the combination at the same time of the localization and the navigation phases presented in section 3.1.

The A-SLAM algorithm relies on the same structure of the navigation filter designed in section 3.1.2, with some slight modifications in order to deal with the dual nature of the problem. In particular, the state vector $\boldsymbol{x}$ of the system (6) and (8) is augmented by including the absolute positions of the fixed modems resolved in the reference system $\{n\}$. Since the dimension $N_m$ of the acoustic network is assumed unknown, the part of the state representing the map is constructed dynamically. The database of the detected modems, initially empty, is updated every time the vehicle receives a measurement from a still unobserved node by adding its absolute position. The equation associated to the map dynamics is thus the following:

$$\dot{\boldsymbol{p}}_{m_i,n} = \boldsymbol{\nu}_{m_i}, \quad i \in \mathcal{V}(t) \subseteq \{1, \ldots, N_m\} \tag{12}$$

where $\boldsymbol{\nu}_{m_i} \sim \mathcal{N}\left(\mathbf{0}, \boldsymbol{Q}_{m_i}\right)$ accounts for the unknown node dynamics and $\mathcal{V}(t)$ denotes the set of the visible node at the time instant $t$. Since the database of the observed nodes is dynamic, the dimension of $\mathcal{V}(t)$ depends explicitly on time and reaches the maximum value $N_m$ when each LBL anchor has provided at least one measurement. The output model in (11) is modified as well to comply with the problem. In particular, the absolute position of the $i$-th acoustic node in equation (11b) is represented in this case by the corresponding components of the state vector:

$$\boldsymbol{y}_{\text{usbl}_\text{i}} = {}^{u}\mathbf{R}_{b}\,{}^{b}\mathbf{R}_{n}(\boldsymbol{\Theta})\left(\boldsymbol{p}_{m_i,n} - \boldsymbol{p}_{n}\right) + \boldsymbol{\eta}_{\text{usbl}} \tag{13}$$

Regarding the implementation, equations (12) and (13) are transformed into the discrete-time ones in order to comply with the previous filtering procedure. When available, a new acoustic measurement is used in the correction step of the filtering algorithm only if the source is already present in the set $\mathcal{V}(k)$. In this case, the predicted state is refined considering among the corrections also the USBL observation. On the other hand, if the measurement comes from a node $m_s$ which was not observed yet, the first acoustic fix is used to initialize the new state variable corresponding to the global position of the new observed node, before adding it to the state space. In the classical approaches that fall in the SLAM framework, this position initialization is generally made in the literature by running some optimal bootstrap algorithms (separated from the main filter) which collect a certain number of measurements to reduce the initial estimation covariance of the new state variable, before adding it to the main filter state space. In the case presented in this work, however, the number of expected fixes per each node is particularly limited (as experimental tests showed), so a fast 1-sample bootstrap phase was employed. First, the refined estimation of the vehicle position $\hat{\boldsymbol{p}}_{n}^{+}(k+1)$ is obtained by running the Kalman correction step using the measurements from the aiding sensors. Then, the USBL measurement from the new node is composed with the vehicle position to obtain the estimated position of the node in the NED frame. Finally, the source $m_s$ is included in the set $\mathcal{V}(k)$ and contextually both the state vector and the covariance matrix of the estimate error are augmented to account for the last detected modem. The new components of the estimates, $\hat{\boldsymbol{p}}_{m_s,n}$ and $\boldsymbol{P}^{+}_{\hat{\boldsymbol{p}}_{m_s,n}}$ are thus initialized respectively with the values:

$$\hat{\boldsymbol{p}}_{m_s,n}(k+1) = \hat{\boldsymbol{p}}_{n}^{+}(k+1) + {}^{n}\mathbf{R}_{b}(\boldsymbol{\Theta}(k))\,{}^{b}\mathbf{R}_{u}\tilde{\boldsymbol{y}}_{\text{usbl}_\text{s}}(k) \tag{14}$$

$$\begin{aligned}\boldsymbol{P}^{+}_{\hat{\boldsymbol{p}}_{m_s,n}}(k+1) =& \boldsymbol{P}^{+}_{\hat{\boldsymbol{p}}_{n}}(k+1) + \\ & {}^{n}\mathbf{R}_{b}(\boldsymbol{\Theta}(k))\,{}^{b}\mathbf{R}_{u}\boldsymbol{R}_{\text{usbl}}\,{}^{u}\mathbf{R}_{b}\,{}^{b}\mathbf{R}_{n}(\boldsymbol{\Theta}(k))\end{aligned} \tag{15}$$

where $\boldsymbol{P}^{+}_{\hat{\boldsymbol{p}}_{n}}(k+1)$ is the sub-matrix of $\boldsymbol{P}^{+}(k+1)$ corresponding to the estimate of the vehicle position. Note that the covariance matrix for the state variable associated with the new node takes into account the updated error covariance of the vehicle position and the covariance of the acoustic measurement, properly transformed using the relative calibration of the sensor with respect to the NED frame axis.

Figure 6. The Typhoon during the CommsNet13 experiment.

## 4. THE TYPHOON AT COMMSNET13

The CommsNet13 experiment has been organized by the NATO CMRE with the main objective to test the performance of several acoustic communication and localization systems using underwater networks. Several teams from different institutions, each one interested in testing several systems, have been involved in the experimentations, held with the support of NRV Alliance. CommsNet13 took place from 2013, Sept. 9$^{\text{th}}$ to 2013, Sept. 22$^{\text{th}}$ in La Spezia and was originally planned in the west area of Palmaria island, Gulf of La Spezia, North Tyrrhenian Sea, where CMRE has a permanent test-bed for underwater networking and communication purposes, namely the LOON (Alves et al., 2012). In CommsNet13, the LOON installation consisted of four EvoLogics modems, placed on the seabed and cable-connected to the shore so that they could be continuously operated and monitored. The role of the Typhoon in this experimentation was to perform both surface and underwater navigation, while trying to localize itself or the other nodes of the network by means of the onboard USBL. The LOON modems were fully compatible with the Typhoon USBL modem, so that the vehicle could use the acoustic measurements to estimate its relative position with respect to the fixed LOON installation. Due to adverse sea and weather conditions in the first week, a preliminary test was carried out within the La Spezia harbour using re-deployable, battery operated, EvoLogics modems as fixed nodes. In the second week the trial was carried out in the open sea close to the LOON area, as originally scheduled. The operating groups have worked in parallel as much as possible, but most of the trials were carried out in series to not interfere the one with the others. The weather constraints and the time-division scheme of the experiment made possible only a limited number of runs, all using TifTu.

Table 1. Definition of the mission waypoints.

| Date | Waypoint | Latitude (°) | Longitude (°) |
|---|---|---|---|
| Sept. 12$^{\text{th}}$ | WP1 | 44.095000 | 9.862050 |
| | WP2 | 44.094300 | 9.859420 |
| | WP3 | 44.093750 | 9.861580 |
| Sept. 22$^{\text{th}}$ | J1 | 44.031890 | 9.830962 |
| | L2 | 44.032116 | 9.828285 |
| | T1 | 44.030610 | 9.829312 |

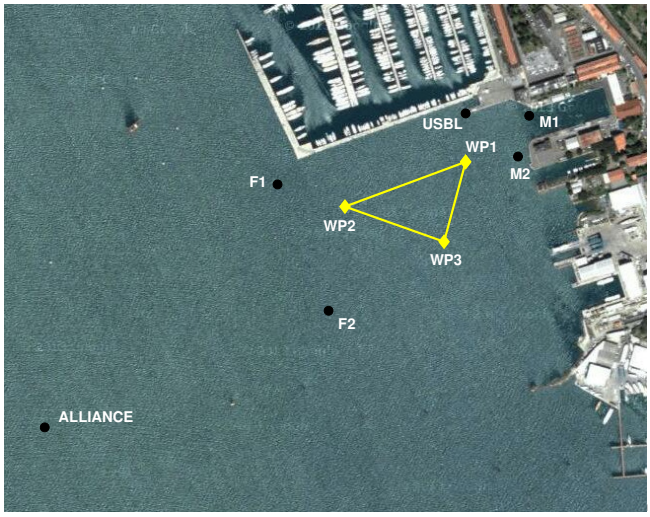


(a) La Spezia harbour, Sept. 12$^{th}$.

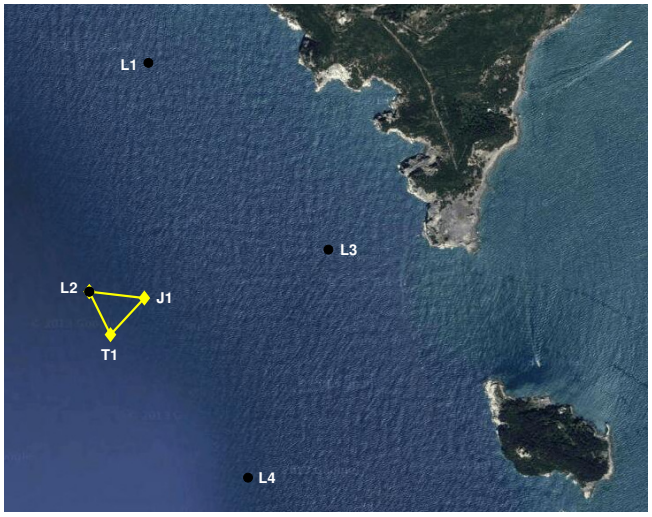


(b) Palmaria Island, Sept. 22$^{th}$.

Figure 5. Mission areas of the two experiments. In Figure 5(b) the modems L1, L2, L3 and L4 constitute the Littoral Ocean Observatory Network (LOON) installation.

The Typhoon trials considered in this work took place on 2013, Sept. 12$^{th}$ and 2013, Sept. 22$^{th}$, both represented in Figure 5. In the first day, the operations were split in two parts. In the morning, Typhoon executed an autonomous mission within the La Spezia harbour, consisting in the repetition of a triangle-shaped path with vertices placed in the waypoints WP1, WP2 and WP3, as shown in Figure 5(a). Starting from waypoint WP1, Typhoon repeated the reference path twice, both on surface. Navigation was performed on the basis of GPS measurements, so that they can be used in post-processing as a ground-truth to evaluate the accuracy of USBL fixes. In the afternoon, Typhoon performed a remotely-operated mission in the same area, travelling along straight lines either on surface or at a constant depth of 3 m and resurfacing before changing direction. In this area, during the whole day, some battery-operated modems, namely M1, M2, F1, F2, USBL and ALLIANCE, were deployed in initially unknown positions. The vehicle can thus exploit the on-board USBL and the ad-hoc installation of fixed nodes to accomplish the localization and navigation tasks. In the second day, Typhoon autonomously travelled along a path on the LOON area, localizing itself with respect to the LOON submerged modem L2 by means of the on board USBL modem. The reference path for the mission, represented in Figure 5(b), was defined through three waypoints respectively called Janus1 (J1), L2 (position of the second one of the four LOON modems) and Typhoon1 (T1). In this run, Typhoon reached J1 from the deployment point, then it travelled three times along the triangle J1-L2-T1-J1: the first and the third times on the surface whereas the second time at a depth of 5 meters surfacing on each waypoint and every two and a half minutes to reset the drift in the position estimation through a GPS fix. In Table 1 the latitude and longitude coordinates of the reference waypoints for both the autonomous missions are reported. Tolerance on waypoints, to consider them achieved, was set to 20 m. The two triangles are between 550 m and 600 m long, both covered with a reference speed of 0.7 m/s. Table 2 summarizes the most important characteristics of the described trials. In particular, the last three columns report some navigation information for each run, i.e. the Typhoon operating modality, the GPS signal availability and the number of USBL measurements. In the following, we will refer to a particular mission using the identifier in the *Alias* column of Table 2.

## 5. EXPERIMENTAL RESULTS

The presented navigation algorithms were tested off-line on the data collected during the missions summarized in Table 2. In order to investigate and compare their performance in different mission scenarios, the outright navigation filters were verified by selecting trials with very different characteristics one from each other, conducted both in the La Spezia harbour and on the LOON installation. In particular, we considered two on-surface missions, 12_M1 and 22_M1, one mixed underwater/on-surface mission constituted by part of both 12_A1 and 12_A2, and finally one completely underwater mission,

Table 2. Typhoon trials summary.

| Date | | Run | Alias | Modality | GPS | # USBL fixes |
|---|---|---|---|---|---|---|
| 2013, Sept. 12$^{th}$ | Morning | 1 | 12_M1 | AUV | ✓ | 25 |
| | Afternoon | 1 | 12_A1 | ROV | ✓ | 27 |
| | | 2 | 12_A2 | ROV | ✗ | 25 |
| 2013, Sept. 22$^{th}$ | Morning | 1 | 22_M1 | AUV | ✓ | 6 |
| | | 2 | 22_M2 | AUV | ✗ | 11 |
| | | 3 | 22_M3 | AUV | ✓ | 3 |

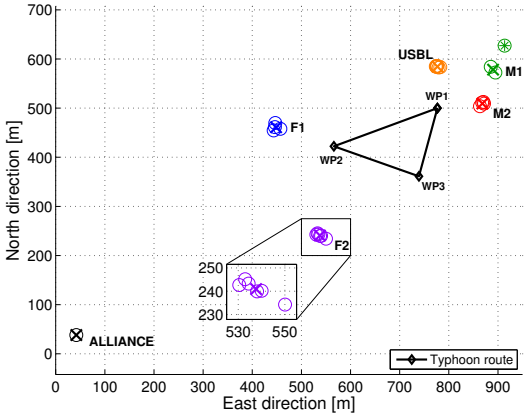


(a) La Spezia harbour, 12_M1 run.

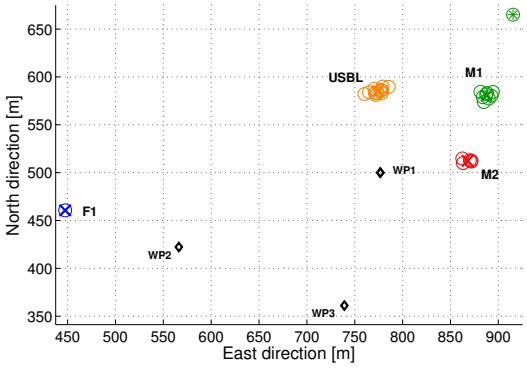


(b) La Spezia harbour, 12_A1 run.

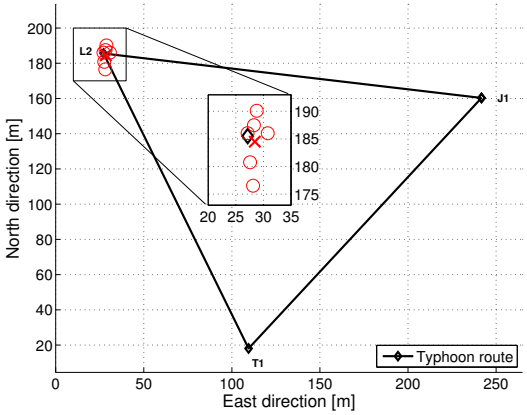


(c) LOON installation, 22_M1 run.

Figure 7. Fixed-nodes localization. Crosses are the final estimates of the modems position. The black path represents the Typhoon predefined route; in 7(b) WP1, WP2 and WP3 are reported only for georeferencing the mission area. In 7(c) the diamond in the enlargement is the actual position of the modem L2 of the LOON. This is the only case in which we had independent ground truth on the modem position. For detailed explanations refer to the text.

22_M2. In the following, we will show some representative outcomes arisen from the execution of both the strategies in the considered mission runs.

### *5.1 Two-phases navigation*

Partial results about the first navigation algorithm have been reported in Caiti et al. (2014a,b).

Figure 7 shows the results for the fixed-nodes localization phase obtained with the data of three different surface trials, namely 12_M1, 12_A1 and 22_M1. The final estimates of the absolute position of the network nodes are indicated with the coloured crosses. Each modem is localized by averaging the rough estimates in the corresponding cluster, represented by the set of circles with the same colour. Note that the mean value of the M1 position is obtained in both the missions 12_M1 and 12_A1 by neglecting an outlier, marked in Figures 7(a) and 7(b) with the starred circles. The enlargements in Figures 7(a) and 7(c) show, as an example, the spatial distributions of the clusters associated to the node F2 and L2, respectively. As can be seen, the elements of each cluster are nearly concentrated in the neighbourhood of their mean value; as a quantification, the estimated standard deviations of the measurements in each set are reported in Table 3. Note that as the dimension $N_i$ of the $i$-th cluster increases, the corresponding estimated standard deviation gets closer to the value representing the instrument precision. Moreover, since the absolute position of the modem L2 in the mission 22_M1 (indicated by the black diamond in the enlargement of Figure 7(c)) is known, we can evaluate the accuracy of the associated estimate, equal to 1.66 m. All the previous considerations highlight thus a precision and an accuracy in the acoustic measurements suitable for the navigation task in the considered application; the estimated standard deviations are also used to tune the filter parameters, in particular the covariance matrix $\boldsymbol{R}_{\text{usbl}}$ associated to the USBL measurements.

Figure 8 shows the North-East path estimated by the acoustic-aided navigation algorithm for the considered mission runs. As can be seen, the filtering algorithm can be split in two different phases. In order to reliably estimate the accelerometers bias and the gain $K_{\text{thr}}$, the navigation filter needs to include some absolute position measurement among the corrections. Since the expected number of acoustic fixes is limited to few tens per run, as Table 2 shows, the GPS measurements are used in the first *initialization* phase (solid green line) as correction feeds to the filter. This way, it is also possible to fix

Table 3. Estimated standard deviations of the USBL. The columns $N_i$ indicate the number of elements of the clusters.

| Source | 12_M1 | | 12_A1 | | 22_M1 | |
|---|---|---|---|---|---|---|
| | $N_i$ | $\sigma$ (m) | $N_i$ | $\sigma$ (m) | $N_i$ | $\sigma$ (m) |
| M1 | 2 | 0.79 | 8 | 4.24 | - | - |
| M2 | 4 | 4.11 | 5 | 3.67 | - | - |
| USBL | 7 | 1.99 | 12 | 6.39 | - | - |
| F1 | 4 | 5.21 | 1 | - | - | - |
| F2 | 6 | 4.55 | - | - | - | - |
| ALLIANCE | 1 | - | - | - | - | - |
| L2 | - | - | - | - | 6 | 4.52 |

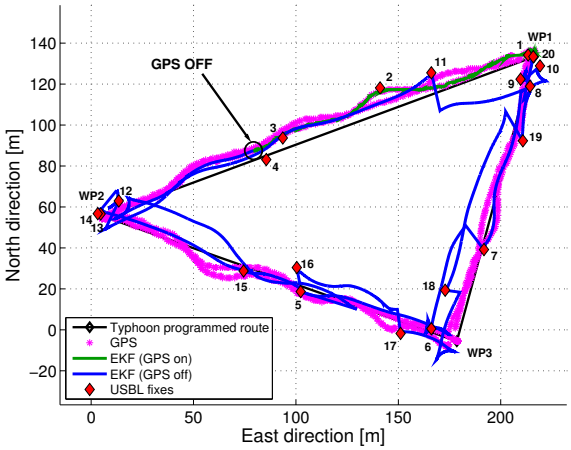


(a) La Spezia harbour, 12_M1 run.

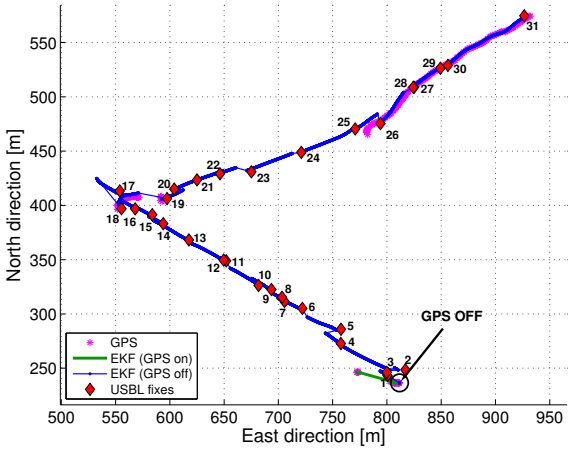


(b) La Spezia harbour, 12_A1 and 12_A2 runs.

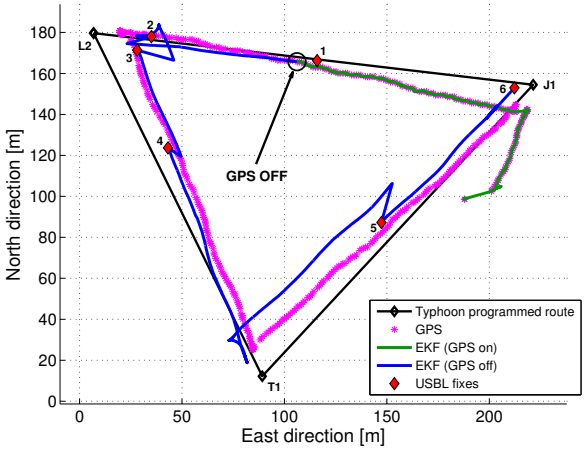


(c) Palmaria Island, 22_M1 run.

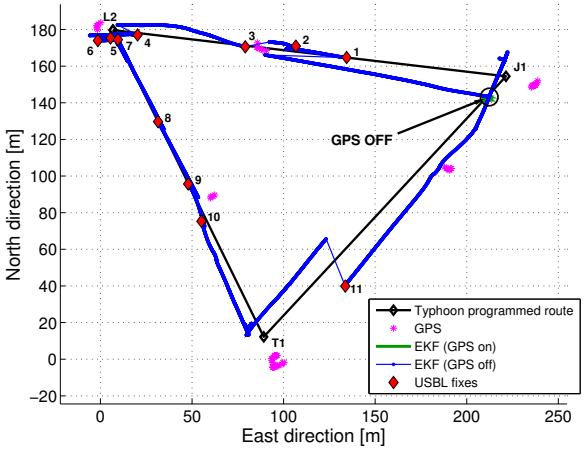


(d) Palmaria Island, 22_M2 run.

Figure 8. Acoustic-aided navigation: estimated North-East path.

the initial conditions for the vehicle position (i.e. to georeference the starting point). A loss in the GPS signal is then simulated from the point marked with a black circle on the map to reproduce the conditions of a normal underwater operation. In this *navigation* phase, represented with the solid blue line, the GPS signal is thus used as *ground truth* only and the absolute vehicle position is refined by using just the USBL measurements, combined with the fixed-nodes positions estimated previously. In Figures 8(b) and 8(d), since there is not a *ground truth* reference during the underwater segments, the jumps in the position estimation due to the USBL measurements are highlighted with a thinner line. The rough corrections for the vehicle position obtained through the acoustic fixes are indicated with the red diamonds. In Figure 9 the norm of the error of the estimated position with respect to the GPS signal is represented for the corresponding mission. The green diamonds indicate the time instants at which a new USBL measurement arrives, showing the effectiveness of the acoustic positioning in keeping the estimation error bounded within reasonable values for the considered application. Moreover, when the acoustic measurements come at a more constant rate, as Figures 8(b) and 9(b) illustrate, the navigation algorithm is able to reduce the estimation error to the value of the GPS precision (approximatively 5 m). It is worth noting that, even with considerable delay between one USBL fix and the next (>3 minutes in cases), the estimation error always remains bounded below 35 m at most and its average is approximatively 10 m. This has to be compared with the expected performance of an industrial grade INS, which, as stated in the introduction, is of the order of 50-60 m at one minute.

As previously pointed out, the GPS signal is necessary at the beginning of the mission to initialize the navigation filter. Moreover, in order to properly make the gain $K_{\text{thr}}$ converge, the vehicle position has to change. It is indeed straightforward from equation (7) that if the vehicle is not moving, i.e. the velocity and the force along the surge axis are both zero, there is a loss in the observability of the system and the gain $K_{\text{thr}}$ is undetermined. This means that if the vehicle is stationary during the initialization phase the gain value remains constant to the initial condition until a position correction, e.g. an USBL fix, arrives while the vehicle is navigating. Figure 10 shows a comparison between the velocity-to-thrust gain estimated using the GPS signal (left) and the USBL corrections (right). The

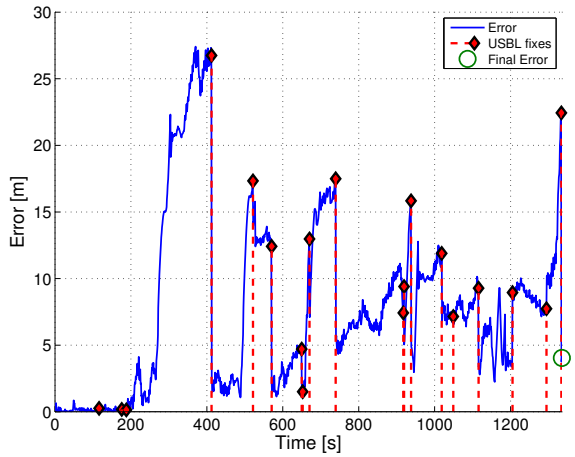


(a) La Spezia harbour, 12_M1 run.

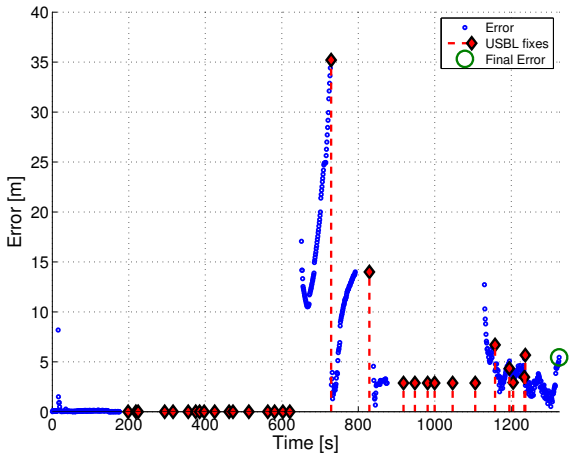


(b) La Spezia harbour, 12_A1 and 12_A2 runs.

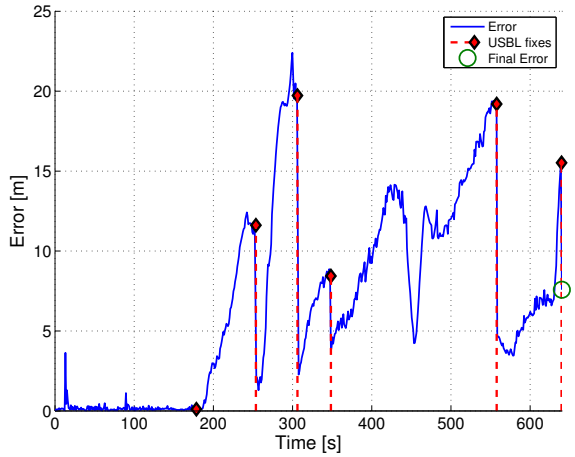


(c) Palmaria Island, 22_M1 run.

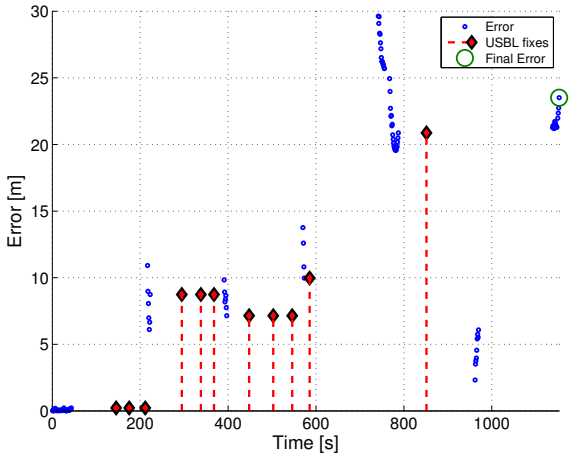


(d) Palmaria Island, 22_M2 run.

Figure 9. Acoustic-aided navigation: norm of the error between the estimated position and the GPS signal.

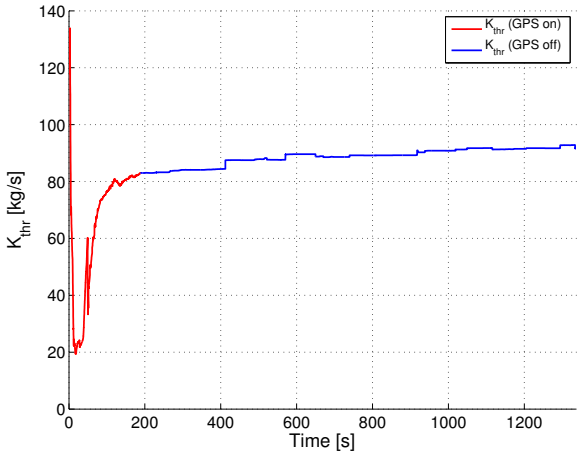


(a) La Spezia harbour, 12_M1 run.

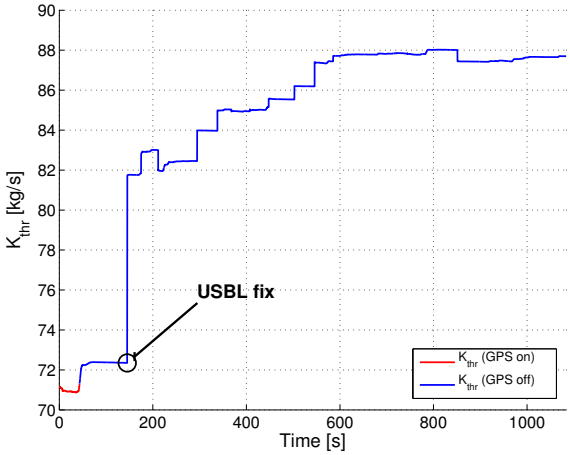


(b) Palmaria Island, 22_M2 run.

Figure 10. Acoustic-aided navigation: comparison between the estimated $K_{\text{thr}}$.

initialization and the navigation phases are indicated with the green and the blue line, respectively. As can be seen from Figure 10(a), in the 12_M1 run the filtering algorithm takes advantage of the GPS measurements during the

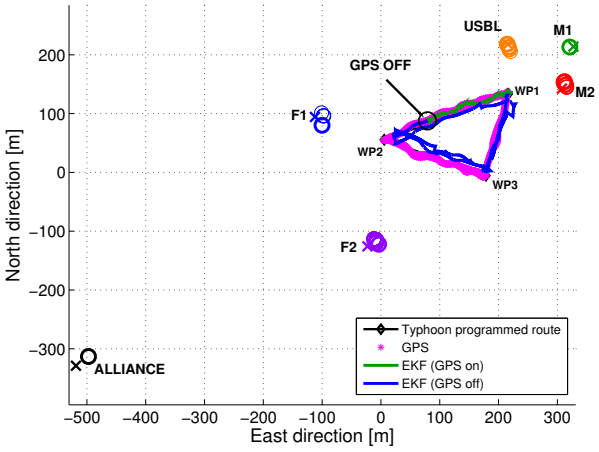


(a) La Spezia harbour, 12_M1 run.

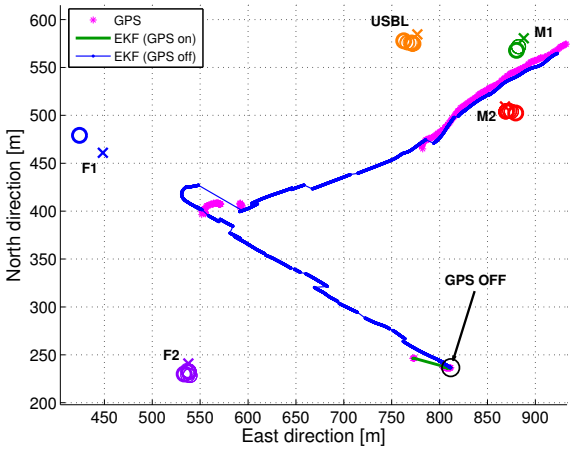


(b) La Spezia harbour, 12_A1 and 12_A2 runs.

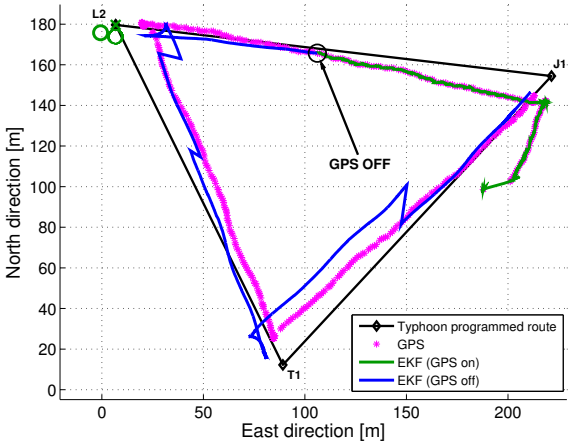


(c) Palmaria Island, 22_M1 run.

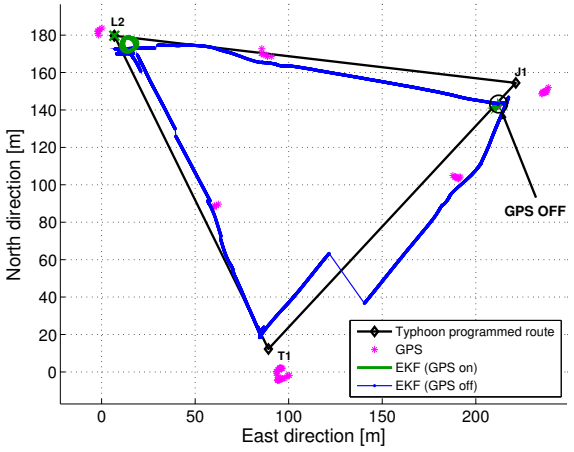


(d) Palmaria Island, 22_M2 run.

Figure 11. Acoustic-based SLAM: estimated North-East path.

initialization phase to estimate the gain $K_{\text{thr}}$ while the vehicle is navigating. On the other hand, in the 22_M2 mission the vehicle dives underwater after about 50 s and the GPS signal becomes unavailable. Furthermore, during the initialization phase the vehicle maintains its position and the navigation filter is not able to estimate correctly the value of the gain, as Figure 10(b) shows. As soon as the first acoustic measurement, indicated with the black circle, arrives (after about 150 s), the estimate of the gain has a discontinuity and slowly converges to the steady-state value with the successive USBL fixes.

Note that in both cases the gain converges after an initial transient approximatively to the same value; the small fluctuations around this steady-state value are due to the different environmental conditions in the two runs (mainly sea currents and sea state).

### *5.2 Acoustic-based SLAM*

Partial results about the A-SLAM algorithm have been reported in Di Corato et al. (2014), addressing the generality of the procedure and its potential to be used in a wide range of AUVs applications.

In Figure 11 the North-East path estimated by the A-SLAM filter for the same mission runs considered previously is shown. The algorithm can be split also in this case in two phases, the initialization and the navigation, with the same representation of Figure 8. The coloured circles represent the estimation of the network topology: in particular, the heavy circles indicate the initial position estimate for each modem, evaluated as in (14). The meaning of the crosses is twofold: on top they indicate the modems position estimated with the localization procedure described in section 3.1.1; on bottom, instead, the green cross represents the actual position of the L2 modem.

Figure 12 shows the localization error for the network nodes with respect to their average (top) or actual (bottom) position value. Figures 12(c) and 12(d) give an account of the estimation accuracy for the L2 modem, which position is known: as can be seen, the final error exhibits a maximum value of about twice the instrument precision reported in Table 3. Finally, it is possible to note how the estimate of each modem begins only after the receipt of the respective first acoustic measurement. As new nodes are observed, the size of the dynamic database increases, reaching eventually the dimension of the network $N_m$.

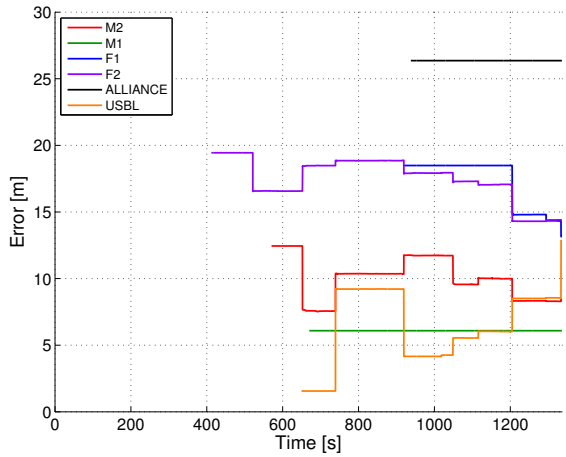


(a) La Spezia harbour, 12_M1 run.

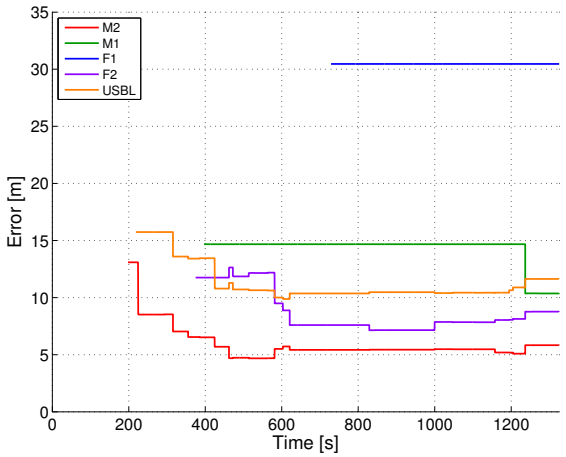


(b) La Spezia harbour, 12_A1 and 12_A2 runs.

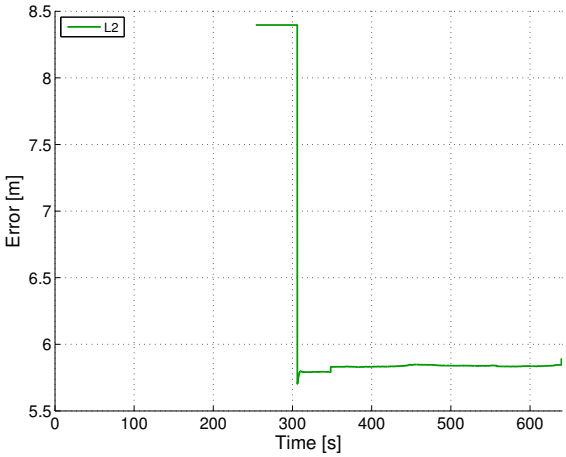


(c) Palmaria Island, 22_M1 run.

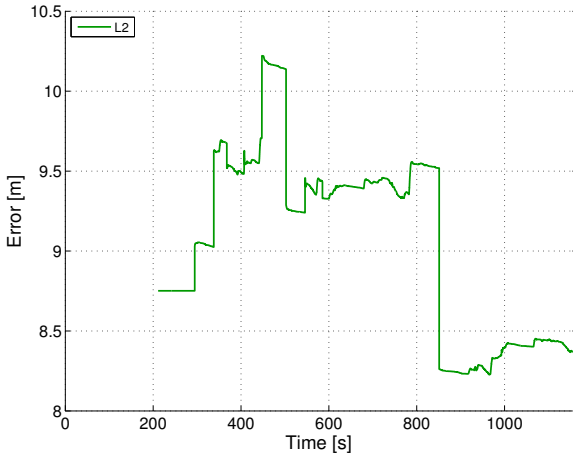


(d) Palmaria Island, 22_M2 run.

Figure 12. Acoustic-based SLAM: norm of the error between the estimated modems positions and their mean (top) or actual (bottom) values.

The error between the estimated vehicle position and the GPS signal reported in Figure 13 highlights performance comparable with those obtained with the previous navigation algorithm. However, since the SLAM procedure corrects the state estimation by exploiting relative position measurements (in this case the USBL ones, modelled in equation (13)), the accuracy of the map estimate and of the vehicle navigation are strongly correlated. For instance, Figures 11(b), 12(b) and 13(b) show that during the mission runs 12_A1 and 12_A2 the vehicle receives an acoustic fix from the modem F1 approximatively at the time instant 700, when the navigation error is about 30 m. As a consequence, the resulting initial condition for the position of the modem F1 has a huge error with respect to the corresponding mean value. Then, the vehicle receives no more measurements from the source F1 and the node position is thus not further refined until the end of the mission. The initialization phase assumes then a prominent role in the algorithm. Indeed, if the gain $K_{\text{thr}}$ is not reliably estimated using the GPS signal as correction, it could not be refined during the navigation phase because the USBL measurements are considered as relative positions. This means that the A-SLAM algorithm could result in large estimation errors and the tuning of the filter parameters would need much more care. In order to verify the performance of the A-SLAM procedure, the USBL and the GPS were thus used in a mutually exclusive way, i.e. the acoustic measurements during the initialization phase were discarded. By combining the relative position provided by the USBL with an absolute, non-divergent information as the GPS position, the A-SLAM algorithm would indeed be able to localize another node within the instrument precision with just one USBL measurement. On the other hand, starting from a rough estimate of the vehicle absolute position, the filter needs more than one acoustic measurement per each node to make the corresponding position estimate converge.

### *5.3 Acoustic performance*

From Table 3, it is possible to note that on 2013, September 12$^{\text{th}}$ the number of fixes from most of the nodes of the fixed installation varies considerably, suggesting a change in the condition of the acoustic channel. In particular, the

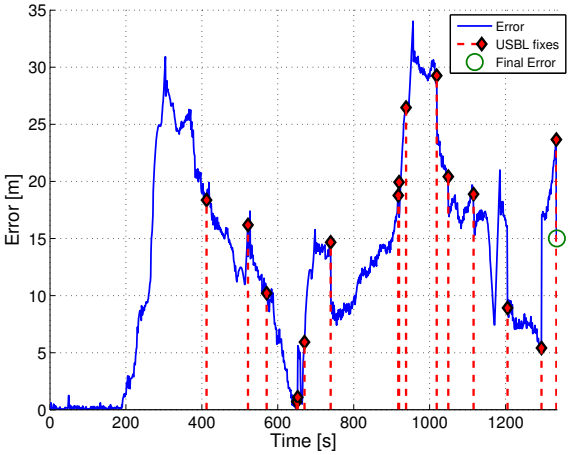


(a) La Spezia harbour, 12_M1 run.

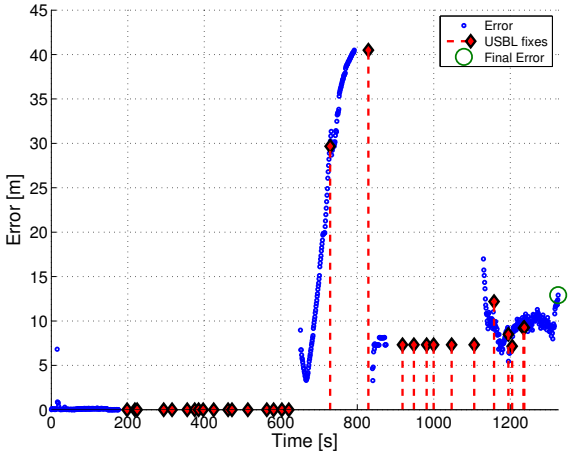


(b) La Spezia harbour, 12_A1 and 12_A2 runs.

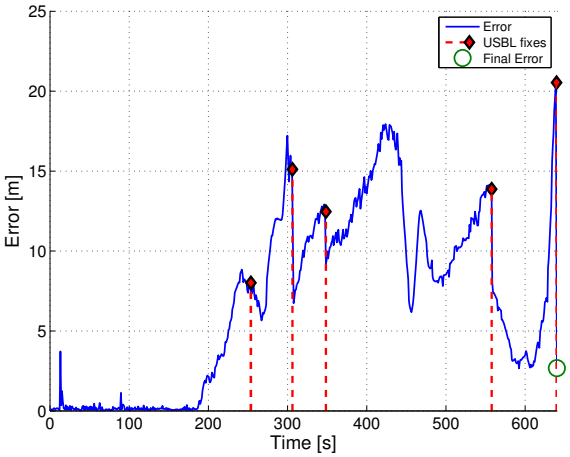


(c) Palmaria Island, 22_M1 run.

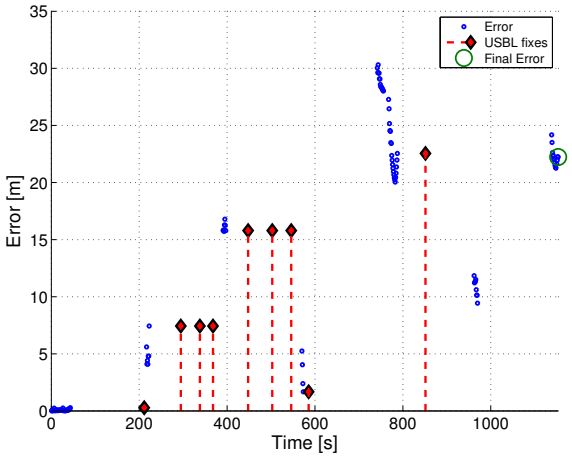


(d) Palmaria Island, 22_M2 run.

Figure 13. Acoustic-based SLAM: norm of the error between the estimated position and the GPS signal.

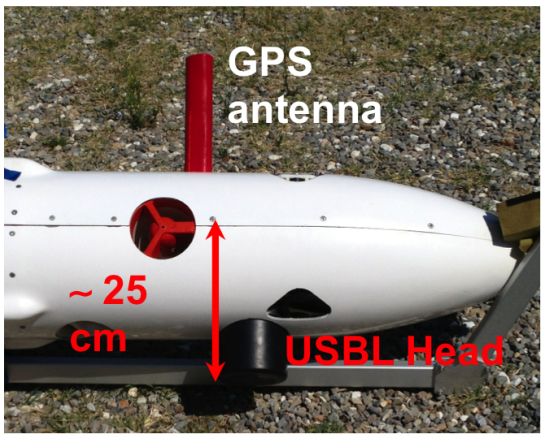


Figure 14. Mounting of the USBL modem on the Typhoon.

measurements received in the afternoon from the nodes M1, and USBL is increased with respect to the morning trial. On the other hand, only one measurement has been observed from F1 and no one from F2 and ALLIANCE. In all the presented trials, the acoustic positioning data come at very irregularly spaced intervals of time during the whole experiment. This is due to different causes: on one hand, the positioning information was embedded in a networked TDMA communication protocol, including round-robin interrogation of all the modems. Moreover, in the missions 12_M1 and 22_M1, with the AUV at the sea-surface, the USBL transponder was about 0.3 m below the sea-surface (as shown in Figure 14), hence suffering from multi-path effects to a much greater extent with respect to what expected in underwater navigation. The combined effect of communication loss due to acoustic channel (variability in time, multi-path effects) and network overburden resulted in intervals between successive acoustic measurements of the order of tens of seconds. Finally, a preliminary analysis on how both the environmental conditions and the experimental set-up affect the traffic of the acoustic positioning information within the network can be done. To this aim, we consider as case study the trials conducted on 2013, September 22$^{\text{th}}$, in which the network was constituted only by the L2 modem. Figure 15 shows the spatial distribution of the modem interrogations: in particular, the green circles and the red crosses indicate the position of the vehicle at the time instant of an acoustic ping, respectively successful or not. A new USBL measurement, indicated

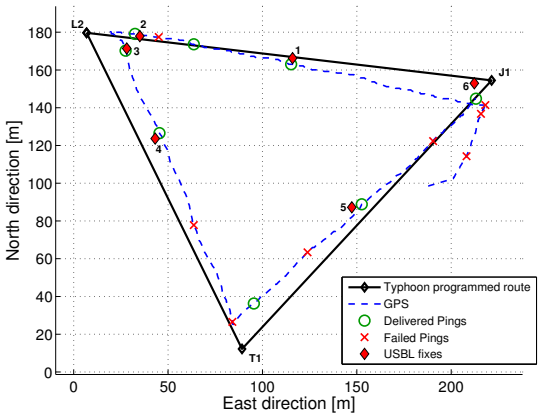


(a) Palmaria Island, 22_M1 run.

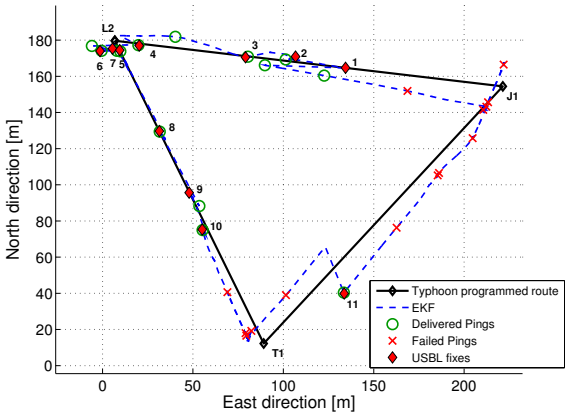


(b) Palmaria Island, 22_M2 run.

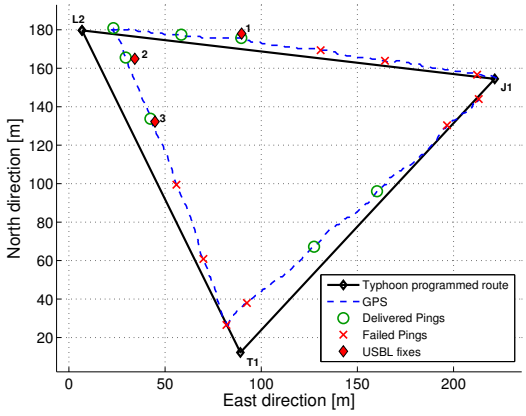


(c) Palmaria Island, 22_M3 run.

Figure 15. Acoustic performance on the LOON installation. The dashed blue line indicates either the GPS position (when available) or the estimated path of the vehicle.

by the red diamond, occurs as a result of a delivered ping; however, it is evident that not all the successful interrogations provide a positioning information. As can be expected, the acoustic communication is strongly dependent on the vehicle position at the moment of the interrogation. We can indeed observe that the number of the successful pings is high in the neighbourhood of the moored modem, while the region between the waypoints T1 and J1 resembles a *shadow zone*. Moreover, as previously pointed out, also the depth of the USBL head has a non negligible influence on the acoustic communication performance: during the surface navigation (Figures 15(a) and 15(c)) the reception of successful measurements is lower than in the underwater travelling (Figure 15(b)). Clearly, this analysis has to be intended as preliminary; extended investigations of acoustic propagation features, based on environmental data collected during the cruise will be the subject of future works.

## 6. CONCLUSIONS

The main features of the Typhoon, a new class of AUVs developed within the THESAURUS project for exploration in team, have been briefly presented. Moreover, two navigation strategies that combine inertial and acoustic measurements by using a mixed LBL/USBL scheme have been developed. The acoustic positioning information is embedded in a networked communication scheme, introducing large delays and overburden. The algorithms has been tested on experimental data collected during the CommsNet13 campaign, led by the NATO CMRE in September 2013, with the Typhoon vehicle.

Results show that even with a low-cost, low-accuracy INS and acoustic positioning information coming at irregularly spaced, time-variant intervals of time, both the procedures are able to keep the navigation error bounded within values suitable for most of the applications of environmental exploration. Following the results achieved, further investigations on the parameter sensitivity (i.e. number of modems deployed, topology of the network, vehicle depth) of the considered localization and navigation scheme will be the subject of future works.

## ACKNOWLEDGEMENTS

This work has been partially supported by the project THESAURUS, PAR FAS Regione Toscana, Linea di Azione 1.1.a.3 (`http://thesaurus.isti.cnr.it`) and by the European ARROWS project, that has received funding from the European Unions Seventh Framework Programme for research, technological development and demonstration under grant agreement no 308724. The help of the NATO Scientific and Technological Organization Centre for Maritime Research and Experimentation (CMRE) for the CommsNet13 experiment is gratefully acknowledged.

## REFERENCES

Allotta, B., Costanzi, R., Meli, E., Pugi, L., Ridolfi, A., and Vettori, G. (2014). Cooperative localization of a team of AUVs by a tetrahedral configuration. *Robotics and Autonomous Systems*, 62(8), 1228–1237. doi:doi:10.1016/j.robot.2014.03.004.

Allotta, B., Pugi, L., Bartolini, F., Costanzi, R., Ridolfi, A., Monni, N., Gelli, J., Vettori, G., Gualdesi, L., and Natalini, M. (2013). The THESAURUS project, a long range AUV for extended exploration, surveilance and monitoring of archeological sites. In *V International*

*Conference on Computational Methods in Marine Engineering (MARINE 2013)*, 760–771.

Alves, J., Potter, J., Zappa, G., Guerrini, P., and Been, R. (2012). A testbed for collaborative development of underwater communications and networking. In *Military Communication Conference, 2012 (MILCOM 2012)*, 1–8. doi:10.1109/MILCOM.2012.6415691.

Batista, P., Silvestre, C., and Oliveira, P. (2012). Ges integrated lbl/usbl navigation system for underwater vehicles. In *Decision and Control (CDC), 2012 IEEE 51st Annual Conference on*, 6609–6614. doi:10.1109/CDC.2012.6426614.

Becker, C., Ribas, D., and Ridao, P. (2012). Simultaneous sonar beacon localization & AUV navigation. In *IFAC Conference on Manoeuvring and Control of Marine Craft*, 200–205. Arenzano, Italy. doi:10.3182/20120919-3-IT-2046.00034.

Caiti, A., Calabro, V., Di Corato, F., Fabbri, T., Fenucci, D., Munafo, A., Allotta, B., Bartolini, F., Costanzi, R., Gelli, J., Monni, N., Natalini, M., Pugi, L., and Ridolfi, A. (2014a). Thesaurus: AUV teams for archaeological search. Field results on acoustic communication and localization with the Typhoon. In *Control and Automation (MED), 2014 22nd Mediterranean Conference of*, 857–863. doi:10.1109/MED.2014.6961481.

Caiti, A., Calabrò, V., Fabbri, T., Fenucci, D., and Munafò, A. (2013). Underwater communication and distributed localization of AUV teams. In *OCEANS '13 MTS/IEEE BERGEN*, 1–8. doi:10.1109/OCEANS-Bergen.2013.6608166.

Caiti, A., Di Corato, F., Fenucci, D., Allotta, B., Bartolini, F., Costanzi, R., Gelli, J., Monni, N., Natalini, M., Pugi, L., and Ridolfi, A. (2014b). Fusing acoustic ranges and inertial measurements in AUV navigation: the Typhoon AUV at CommsNet13 sea trial. In *OCEANS '14 MTS/IEEE TAIPEI*, 1–5. doi:10.1109/OCEANS-TAIPEI.2014.6964559.

Carlton, J. (2012). *Marine propellers and propulsion*. Butterworth-Heinemann, third edition.

Di Corato, F., Caiti, A., Fenucci, D., Grechi, S., Novi, M., Pacini, F., and Paoli, G. (2015). Optimal aided inertial navigation, augmented with inter-sensors self-calibration. In *OCEANS '15 MTS/IEEE GENOVA*.

Di Corato, F., Fenucci, D., Costanzi, R., Monni, N., Pugi, L., Ridolfi, A., Caiti, A., and Allotta, B. (2014). Toward underwater acoustic-based simultaneous localization and mapping. experimental results with the Typhoon AUV at CommsNet13 sea trial. In *OCEANS '14 MTS/IEEE ST.JOHN'S*. St. John's, Canada. doi:10.1109/OCEANS.2014.7003092.

Fossen, T.I. (1994). *Guidance and control of ocean vehicles*. John Wiley and Sons, first edition.

Furfaro, T. and Alves, J. (2014). An application of distributed long baseline - Node ranging in an underwater network. In *Underwater Communications and Networking (UComms), 2014*, 1–5. doi:10.1109/UComms.2014.7017126.

Indiveri, G. (2013). An outlier robust filter for maritime robotics applications. *Paladyn, Journal of Behavioral Robotics*, 4(4), 196–203. doi:10.2478/pjbr-2013-0012.

Jazwinski, A.H. (2007). *Stochastic processes and filtering theory*. Courier Dover Publications.

Kinsey, J. and Whitcomb, L. (2007). In situ alignment calibration of attitude and doppler sensors for precision underwater vehicle navigation: Theory and experiment. *Oceanic Engineering, IEEE Journal of*, 32(2), 286–299. doi:10.1109/JOE.2007.893686.

Morgado, M., Oliveira, P., and Silvestre, C. (2013). Tightly coupled ultrashort baseline and inertial navigation system for underwater vehicles: An experimental validation. *Journal of Field Robotics*, 30(1), 142–170. doi:10.1002/rob.21442.

Newman, P. (2003). The MOOS - cross platform software for robotics research. URL `http://www.robots.ox.ac.uk/%7Emobile/MOOS/wiki/pmwiki.php`.

Paull, L., Saeedi, S., Seto, M., and Li, H. (2014). AUV navigation and localization: A review. *Oceanic Engineering, IEEE Journal of*, 39(1), 131–149. doi:10.1109/JOE.2013.2278891.

Petillot, Y., Maurelli, F., Valeyrie, N., Mallios, A., Ridao, P., Aulinas, J., and Salvi, J. (2010). Acoustic-based techniques for autonomous underwater vehicle localization. *Proceedings of the Institution of Mechanical Engineers, Part M: Journal of Engineering for the Maritime Environment*, 224(4), 293–307. doi:10.1243/14750902JEME197.

Rogers, R.M. (2000). *Applied Mathematics in Integrated Navigation Systems*. American Institute of Aeronautics and Astronautics, third edition.

Tang, K., Wang, J., Li, W., and Wu, W. (2013). A novel ins and doppler sensors calibration method for long range underwater vehicle navigation. *Sensors*, 13(11), 14583–14600. doi:10.3390/s131114583.

VectorNav Technologies LLC, . (2014). VectorNav support library. URL `http://www.vectornav.com/support/library?id=33`.

Webster, S.E., Eustice, R.M., Singh, H., and Whitcomb, L.L. (2012). Advances in single-beacon one-way-traveltime acoustic navigation for underwater vehicles. *The International Journal of Robotics Research*, 935–950. doi:10.1177/0278364912446166.

**Benedetto Allotta** Ph.D., is Full Professor of Robotics and Mechanical Design at the School of Engineering of the University of Florence, Italy. He is cofounder and coordinator of the Laboratory of Mechatronics and Dynamic Modelling (MDM Lab). His current research interests are underwater robotics, sensor-based navigation of vehicles, Hardware in the Loop (HIL) simulation, and automation in transport systems. He is author of about 200 publications, including more than 40 papers in International Journals with peer review.

**Fabio Bartolini** is a Ph.D. Researcher (Assistant Professor) of Machine Theory with the School of Engineering, Department of Industrial Engineering, University of Florence, Italy. His current research interests include mechanical design, mechatronics, and underwater robotics.

**Andrea Caiti** is Full Professor of Automatic Control at the University of Pisa, Italy. He has previously held positions as a Staff Scientist at the NATO SACLANT Undersea Research (currently CMRE) and as adjunct, assistant and associate professor at the Universities of Genova, Pisa and Siena, respectively. He was the Director of the Inter-university Research Centre on Integrated Systems for the Marine Environment (ISME) from 2001 to 2008, and is currently Coordinator of the Ph.D. Pro-

gramme in Automation Robotics and Bioengineering at the University of Pisa. His research interests are in the field of oceanic engineering, underwater robotics, marine acoustics. He has published more than 70 peer reviewed journal papers or book chapters, and more than 150 contributions to conference proceedings.

**Riccardo Costanzi** received his Ph.D. from the University of Florence, school of Engineering, in 2015. His research activity is focused on underwater robotics with particular attention to navigation and control systems for Autonomous Underwater Vehicles.

**Francesco Di Corato** received the Ph.D. degree in automation, robotics, and bioengineering from the University of Pisa in 2013. He was a Postdoctoral Student at the Inter-university Center on Integrated Systems for the Marine Environment, University of Pisa unit (2012-2015). Currently he is Resident Engineer CTO at the Joint Development Centre (Magneti Marelli - VisLab).

**Davide Fenucci** received the B.Sc. degree in computer science engineering and the M.Sc. degree in automation engineering from the University of Pisa, Pisa, Italy, in 2009 and 2012 respectively. Since 2013 he is a Ph.D. student in ICT, robotics and automation engineering at the University of Pisa.

**Jonathan Gelli** is a Ph.D. Student of Machine Theory and Robotics with the School of Engineering, Department of Industrial Engineering, University of Florence, Italy. His current research interests include mechanical design, mechatronics, and underwater robotics.

**Piero Guerrini** received the Master Degree in Electronic Engineering from the University of Genova in 1978. Since 1981 he has been working in the Electronic Engineering Department of the NATO STO Ctr. for Maritime Research and Experimentation (CMRE) in La Spezia, at the time named SACLANT ASW Res. Ctr. Through the years, he has worked in the design, development and testing at sea of many innovative instrumentation for ocean acoustics, geophysics and oceanography applications.

**Niccol Monni** is a Ph.D. Student of Machine Theory and Robotics with the School of Engineering, Department of Industrial Engineering, University of Florence, Italy. His current research interests include mechanical systems modelling, robotics, and underwater robotics.

**Andrea Munaf** received the Ph.D. degree in automation,robotics, and bioengineering from the University of Pisa, Pisa, Italy, in 2009. He worked as a Postdoctoral Student at the Inter-university Center on Integrated Systems for the Marine Environment (ISME), University of Pisa unit, from 2009 to 2013. He is currently a Research Scientist at the NATO STO Ctr. for Maritime Research and Experimentation (CMRE).

**Marco Natalini** received his B.Sc. degree in electronic engineering at the University of Florence. He is currently a technical consultant of the Department of Industrial Engineering, University of Florence, Italy. His skills address electronics, mechatronics, and underwater robotics.

**Luca Pugi** is a Ph.D. Researcher (Assistant Professor) of Machine Theory and Mechatronics at the University of Florence, School of Engineering. His main research activities deal with Vehicle Dynamics, Mechatronics, including Electric and Fluidic Systems.

**Alessandro Ridolfi** is a Ph.D. Researcher (Assistant Professor) of Machine Theory and Robotics with the School of Engineering, Department of Industrial Engineering, University of Florence, Italy. His current research interests include vehicle dynamics, mechanical systems modelling, robotics, and underwater robotics. He is also an Adjunct Professor of the Syracuse University in Florence, teaching Dynamics.

**John R. Potter** received his Ph.D. from the Dept. Applied Mathematics & Theoretical Physics, University of Cambridge, UK. After a period with the British Antarctica Survey, in 1986 he joined the SACLANT Undersea Research Ctr. (currently CMRE) in La Spezia, Italy, as a scientist in the acoustical oceanography group. He then held positions at Scripps Oceanographic Institution, San Diego, CA (1991-95), and at the National University of Singapore (1995-2007), where he founded and directed the Acoustic Research Lab. In 2008, he came back to La Spezia at NATO STO Ctr. for Maritime Research and Experimentation (CMRE), where he is currently a Principal Scientist in the Strategic Development Office.